

DETERMINING INDICIES OF REFRACTION FOR ThO₂ THIN FILMS

SPUTTERED UNDER DIFFERENT BIAS VOLTAGES

FROM 1.2 TO 6.5 eV

BY SPECTROSCOPIC ELLIPSOMETRY

William R. Evans* and David D. Allred*⁺

*Brigham Young University, Provo, UT

⁺allred@byu.edu; phone: (801) 422-3489; www.physics.byu.edu/faculty/allred/cv/05CV.htm

Abstract

We used spectroscopic ellipsometry to determine the optical constants of seven ThO₂ thin-film samples, thickness ranging between 28 and 578 nm, for the spectral range of 1.2 to 6.5 eV. The samples were deposited by biased radio-frequency sputtering at DC bias voltages between 0 and -68 V. The index of refraction, n , does not depend on bias voltage, sputter pressure, deposition rate, or thickness. Specifically, the value of n at 3 eV is 1.86 ± 0.04 for the unbiased samples and 1.86 ± 0.04 for the biased samples. The average value of n at 3 eV for the thicker samples ($d \geq 50$ nm) was 1.87 ± 0.05 , and 1.85 ± 0.02 for the thinner samples ($d \leq 50$ nm).

Introduction

Determining the optical properties of thoria (thorium dioxide - ThO_2) is important for technological as well as for basic science reasons. Thoria is the most refractory oxide known. Its melting temperature is above 3500K. It, with nonnuclear CeO_2 , and the important nuclear oxides, UO_2 and PuO_2 constitute the oxides with the fluorite structure. However, it is the only one of the four with a stable +4 oxidation state. It has a number of nonnuclear uses including some which rely on its visible and near UV optical transparency, including optical coatings[1], and cathodoluminescence. It is the primary material in Welsbach gas mantles which are widely used in portable camping lanterns. There is also an interest in understanding the optical properties of the oxides and fluorides of heavier group IV metals related to their capacity to act as hosts to rare earth and transition metal ions. These have applications as gamma radiation detectors and phosphors. This has led to many experimental[2] and some computational studies.[3] In addition being the only stable oxide of thorium, the surface of thorium metal and many thorium alloys in oxidizing ambients can be expected to be coated with thoria which will influence the apparent optical properties of the metal. Considering how important thorium and thoria are and how much they have been studied in the past half century, it is surprising that the optical constants of thoria are not better known. In fact, there has been no general agreement on the band gap of thoria; some studies placing the absorption edge near 4 eV. Others place it near 5.9 eV.[4-6] We discuss the band gap of ThO_2 in another publication.[7]

In addition to these applications, recently, thin-film thoria has been investigated as a reflector for the extreme ultraviolet (EUV) and soft x-rays. Its low angle reflectance is twice as high as standard materials at about 200eV.[8] Progress in this area is limited, however, by a lack of knowledge of the properties of the deposited materials including film thickness and density. An understanding of factors that can affect the characteristics of the thin film during deposition is central to this knowledge. We here report on the effect of bias voltage on the index of

refraction for reactively sputtered ThO₂ thin films, deposited by radio-frequency sputtering. Many optical materials have lower index as thin film. This has been related to density. Bias sputtering has been used to increase the density of insulating optical thin films such as silicon nitride.[9] Knowing the index of this material makes it possible to determine the thickness of the layers which are used in EUV and soft x-ray studies or which form on thorium surfaces. Learning how to densify the material could lead to higher reflectances.

Experimental

The thorium oxide samples were deposited via reactive, radio-frequency (RF), magnetron sputtering using a US Inc. Mighty Mak 4-inch gun, powered with a Plasmatherm 3 kW RF power supply. The incident power was set to about 300 W and there was about 20 W of reflected power once the plasma lit. The base pressure of the turbopumped (4 inch) and cryopumped (CryoTorr 8) Cu-gasketed, high vacuum chamber was less than about 1×10^{-2} Pa (0.1 mtorr).

Both high vacuum pumps were used during the depositions. The gate valve in front of the cryopump was manually controlled to be almost shut. The turbo was run full open. The working gas composition was a mixture of argon and oxygen, normally at a total pressure of about 1.1-1.3 Pa (8-10 mtorr). The oxygen flow was controlled by a sapphire leak valve and was set to about 0.33 Pa (2.5 mtorr) using the system's ion gauge before the Ar (99.999%) was introduced. Under these conditions the normal deposition rate was about 1 nm/min. A 101-mm diameter, 6.5-mm thick thorium target, previously cut from a cast thorium ingot, was used in a sputter-up geometry. The target-to-substrate distance was about 0.25 m. A moveable shutter lay 5.5 cm below the substrate.

The deposition substrates were silicon wafer pieces from standard polished silicon wafers (100 orientation) and pieces broken from synthetic, fused quartz slides (G. Finkenbeiner, Inc. 781 899-3138) chosen to possess high UV transmission at 6.5 eV. Atomic Force Microscopy

(AFM) measurements have shown the typical rms roughness of similar wafers to be ~ 0.2 nm over a $100\text{ nm} \times 100\text{ nm}$ area. The thickness of the native silicon dioxide of the silicon wafers used was estimated to be 2.0 nm, which we found to be the average for similar wafers.

The samples were suspended upside-down above the sputter gun. The sample holder was attached to a 9.5 mm Cu-post (Ceramaseal™) feed through (on a 2.75-in conflat). This allowed the substrates to be connected to a negative bias voltage and be isolated from the rest of the chamber. Samples were sputtered at bias voltages between 0 and 75 V. Bias current was also measured and was typically about 0.5 A. We were certain that bias current was present, because on some of our earlier samples, sparking occurred when the bias current got too high.

The deposition system had a quartz-crystal monitor positioned to see most of the flux which struck the substrates and was not blocked by the shutter which protected the sample holder until the sputter rates were stabilized. This allowed us to achieve the approximate film thickness desired. We obtained a more accurate measurement of each film's thickness using low-angle x-ray thin-film interference. Following each deposition we measured the low-angle ($\sim 0.6^\circ$ - 1.8° (2 θ)) x-ray reflection (XRR) spectrum of the reflectance sample, using a Scintag® model XDS 2000 X-ray Diffractometer, with Cu-K α radiation (0.154 nm). To determine the thickness of the ThO $_x$ layers we compared the observed position of interference minima in the measured XRR spectrum with those modeled for a range of Th thicknesses on 2 nm of SiO $_2$ (typical thickness of native oxide) on Si substrates. Bissell et al discuss this process in more detail.[10]

We also measured the x-ray scattering of the two thickest films over the range 15° to 90° (2 θ) to ascertain the crystallinity of the films.

Figure 1 shows the counts per second of scattered x-rays at each angle between 15° and 87° (2 θ) by XRD from sample ThO $_2$ 050604-2 (thickness = 357 nm) with the background removed. The first vertical set of values above each peak provides the peak position data, with the middle entry being the distance between lattice planes in angstroms. The second line of

values shows the standard positions and relative intensities of the peaks for ThO₂, as provided by the *Powder Diffraction File*[11], with the indices for the appropriate lattice planes shown in parentheses. The notation accompanying each peak is the relative intensity of each of the peaks as obtained by a numerical summation over the range of the peak, normalized to intensity of the first peak. This data provides firm evidence that the film is polycrystalline ThO₂ with preferred orientations in the (111) and (110) directions. The (100) and similar low-angle orientations are largely absent.

The composition of one of the samples was also measured using x-ray photoelectron spectroscopy (XPS). The XPS system at BYU is equipped with a small sputter gun which removes the film over a small area on the sample. This enables us to determine composition with depth. The graph in Figure 2 indicates percent composition as a function of sputtering time (precise translation from sputtering time to depth is not possible) as determined by XPS. Ellipsometric fitting placed the thickness of this sample as 350 nm. The films give a Th to O ratio of approximately 1 to 2 throughout the thickness of the sample, as we would expect for ThO₂.

Surface roughnesses of our films were measured using a Veeco Instruments Dimension 3100 Atomic Force Microscope at Brigham Young University. The surface roughness, measured on a 1-micron by 1-micron area and averaged over two spots on each of four samples, was 5.1 ± 0.4 nm and was independent of thickness. This value for roughness was used in modeling the films' ellipsometric data. Figures 3a and 3b show the surface topography from the films 050818 and 050604-2, which are 578 and 357 nm thick, respectively. (See Table I).

Optical properties of our thin films were measured using a John A. Wollam Company M2000 Spectroscopic Ellipsometer. Ellipsometric reflectance data (Ψ and Δ) was taken on the silicon samples at energies between 1.24 and 6.5 eV, and at angles between 67° and 83°, taking measurements every degree. The ellipsometer at BYU is also set up to take normal incidence

transmission measurements. We took normal incidence transmission measurements over the same energy range on the samples deposited on quartz. Optical constants were then modeled using the WVASE software provided with the ellipsometer. We modeled the silicon samples with a 1 mm Si layer, under a 2 nm SiO₂ layer, followed by the ThO₂ layer whose optical constants we were modeling. Then a layer of roughness, set at the root mean squared value determined by AFM. The thickness of the ThO₂ layer was initially set at the value found by XRD, but then we allowed it to vary somewhat. This was done because fits done, without allowing the thickness to change, were visibly and quantitatively (larger error term) poor. We were able to achieve (see Table I) a “mean square error” (roughly equivalent to χ^2) of less than 2.5 for the modeled optical constants in all but the thickest samples. This means that the model fit to the data is as good as possible. The measurement is very over-determined, since the model has only 9-11 parameters, whereas the thousands of points of data are collected for each sample.

Reported Data and Discussion

The fit values of n at any energy mostly lie within a narrow range. That is, the general shapes of the different fits of n are essentially the same up until about 6.0 eV. It is at higher energies the ellipsometer loses sensitivity. Above about 5.5 eV, some curves climb more steeply than others. Around 3.0 eV the index of refraction is about 1.86 ± 0.05 .

In Figure 4, the values of n fit for seven different samples are plotted against photon energy. In the legend of the graph in Figure 5, we have listed the thickness to which each sample was sputtered and the bias voltage at which it was sputtered. Note that this graph only shows data between photon energies of 3 and 5 eV, which is only a partial range. Data are shown for an energy range of 1.2 to 6.5 eV in Figure 4. This graph uses a reduced energy range to magnify the differences between the curves. These values fall into three different bands between 3 and 5 eV. However, we do not see a correlation between into which band a sample falls, and at what

bias voltage the sample was sputtered. The non-dependence of n on bias voltage is better illustrated in Figure 6.

We found no correlation of n with bias voltage, sputter pressure, deposition rate, or any other deposition parameter monitored. The average value of n at 3 eV was 1.86 ± 0.04 for the unbiased samples, and also 1.86 ± 0.04 for the biased samples. These standard deviations were calculated from the best WVASE fits of n for the set of samples in each category. Similarly, we do not see a difference in n between the thick and thin samples. The average value of n at 3 eV was 1.87 ± 0.05 for the thicker samples ($d \geq 50$ nm), and 1.85 ± 0.02 for the thinner samples ($d \leq 50$ nm).

The WVASE software does not provide the error bars associated with each of the obtained $n(E)$ curves. The standard deviations across different samples as shown in Figure 5 give a good idea of the relative errors. WVASE provides instead error bars associated with each of the fitting parameters (see Table I). These include the positions and magnitudes of the different poles. Translating these into uncertainties in the values for $n(E)$, which are determined from these parameters, might be done using a type of *Monte Carlo* method, which would consist of varying each of the parameters within the confidence interval and measuring the amount of variation in n . This, however, was outside the scope of this report.

There does not seem to be a significant correlation between the sputtering bias voltage, and the value of n . Bias voltage cannot be reliably expected to increase the index of refraction of our ThO₂ thin films.

The data we obtained compare well with that of Liddell[12] who studied how to determine the optical constants of several different weakly absorbing oxides from reflection and transmission. Her films were deposited using electron-bombardment evaporation onto synthetic silica substrates (Spectrosil B). Her values of n for ThO₂ were fit assuming a homogenous film of thickness 92.4 nm. We find that the values of n she reports lie on, or close to the middle of,

the curves that we plot in Figure 4. On the other hand, the values from the other reports of thin films have higher values of n . Thoria films from ref. 1 had values of $n(3.1 \text{ eV}) = 1.96\text{-}2.00$ and 2.03 for films prepared with thorium nitrate and thorium chloride, respectively, and annealed at 873 K . Annealing at 873 K removed nitride or chloride ions to about 1.5% . Mahmoud[13] reports n for films prepared by sol gel, to have values of $n=1.92, 1.94, 1.98$ and 2.07 for $2.48, 2.76, 3.1$ and 3.54 eV , respectively, (data drawn from Fig. 7 of ref.13) compared to $1.83, 1.85, 1.87,$ and 1.89 our films. Our films are significantly less dispersive than Mahmoud's. Much of the increase he saw may be due to the fact that these points are near to the absorption edge of his material.[13]

The index of bulk thoria in the visible is 2.2 . [14] Assuming that this is the proper index for thin films as well and their apparent lower index is due to voids, we employed effective media theory for dielectric constants [15] to calculate that the approximate void fraction spherical voids in thoria with an apparent index of 1.82 , is about 30% . Other techniques for densifying thoria films, such as depositing at higher temperatures, ion beam bombardment, or biased AC sputtering, need to be explored. Since thoria has such a high melting point, when it is deposited at room temperature, its structure can be expected to be Zone 1, which is characteristically porous.

Turning now to the determination of k , we observed that the fitting of n and the fitting of k could be conducted relatively independently. We proceeded in this way. The first fit was for ellipsometric Ψ and Δ values measured for the film deposited on silicon, fitting n , assuming no k . Then we fit k to the transmission data from the samples on quartz, using the obtained values of n , first point-by-point, and then using a Tauc-Lorentz oscillator model.[16] The second fit on silicon was a fit of n using the values of k we obtained from the transmission data. We found that between the two fits on the same silicon sample with the addition of absorption, the values of n that we obtained did not change significantly. This is shown schematically in Figure 7.

We note that adding k between the first and second fits on silicon did not change the values of n significantly. Therefore, it appears that the values of n are not greatly dependant on the presence of k , *when k is small*. These indications give us confidence that our results for each of n and k are mutually independent.

Conclusions

We have achieved new milestones in our understanding of the optical properties of reactively sputtered ThO₂ in thin film form, satisfactorily evaluated the deposition technique of biased RF magnetron sputtering, and established procedures for determining the optical constants of thin films in the visible by means of spectroscopic ellipsometry. Biased DC sputtering cannot be reliably expected to alter the indices of refraction of ThO₂ thin films deposited by RF magnetron sputtering.[17]

Acknowledgements

A BYU ORCA Scholarship to William Evans and BYU Department of Physics and Astronomy research funds aided in the research. We also acknowledge gratefully the financial contributions of V. Dean and Alice J. Allred and Marathon Oil Company for gifts to Brigham Young University for thin-film research. We thank all the members of the BYU EUV team for their support, especially Amy Baker for XPS, Jed Johnson for advice in sputtering films and Michael Clemens for AFM.

Comment [MD1]: (Other support and funding.)

References

- [1] A. I. Sviridova, and N. V. Suikovskaya, *Optics and Spectroscopy*, **22** (1967) 509.
- [2] R.C. Linares, *J. Phys. Chem. Solids*, **28** (1967) 1285.
- [3] J.F. Rivas-Silva, J.S. Durand-Niconoff, M. Berrondo, *Computational Materials Sci.*, **18** (2000) 193-198.
- [4] See, for example. Trevor R. Griffiths, and James Dixon, *J. of Chemical Society, Faraday Transactions*, **88**, (1992) 1149, and ref. cited within, especially ref. 2-9.
- [5] Elward T. Rodine and Peter L. Land, *Phys Rev. B* **4** (1971) 2701, and ref. cited within. Also PhD dissertation: Elward Theodore Rodine, *Thermoluminescence of Thorium-Oxide Single Crystals*, University of Nebraska–Lincoln (1970); at <http://digitalcommons.unl.edu/dissertations/AAI7103654/>
- [6] Trevor Griffiths, and James Dixon, *Inorganica Chimica Acta*, 300-302 (2000), 305.
- [7] W.R. Evans, and D.D. Allred, in: Ali M. Khounsary, and Christian Morawe, (Eds.) *Advances In X-Ray/EUV Optics, Components, And Applications*, **6317**, *Proceedings of SPIE*, (2006) submitted.
- [8] Jed E. Johnson, David D. Allred, R. Steven Turley, William R. Evans, and Richard L. Sandberg, in: Sarrao, A. Schwartz, M. Antonio, P. Burns, R. Haire, H. Nitsche (Eds.) *Actinides—Basic Science, Applications, and Technology*, vol. 893, Material Research Society Symposium Proceedings, 2005, in press
- [9] See, e.g. Joo Han Kim and Ki Woong Chung, *J. Appl. Phys.* **83**, (1998) 5831.
- [10] L. J. Bissell, D. D. Allred, R. S. Turley, W. R. Evans, J. E. Johnson, in Regina Soufli, and John F. Seely (Eds.), *Optical Constants of Materials for UV to X-Ray Wavelengths*, **5538**, *Proceedings of SPIE*, Bellevue, WA, 2004, 84.
- [11] *Powder Diffraction File*, (Joint Committee on Powder Diffraction Standards, Philadelphia, PN, 1960), Inorganic, Sets 1-5, p. 527. Index number 4-0556.
- [12] H. M. Liddell, *J. Phys. D: Appl. Phys.*, **7**, (1974) 1588.
- [13] S. A. Mahmoud, *Solid State Sciences*, **4** (2002) 221.
- [14] Richard C. Anderson, in Allen M. Alper (Ed.), *The High Temperature Oxides*, Academic Press, Inc., NY, 1970, p 22.
- [15] F.L. Galeener, *Phys. Rev. Letters*, **27** (1971) 421.
- [16] *Guide to Using WVASE32*. J.A.Wollam Co., Inc. p.E-2, E-13, E-21.
Citing: G.E.Jellison, Jr. and F.A. Modine, “Parameterization of the optical functions of amorphous materials in the interband region,” *Appl. Phys. Lett.* **69**, 371 (1996), Erratum, *Appl. Phys. Lett.* **69**, 2137 (1996). for the Tauc-Lorentz Oscillator material.

Comment [MD2]: {year???

Comment [MD3]: {Is this citation ok???

- [17] W.R. Evans, Honors Thesis (Brigham Young University, December 2005), available at <http://www.physics.byu.edu/faculty/allred/cv/Theses/WRE/Bill's%20ThO2%20Ellipsometry%20Thesis%20--%2017%20Oct%202005.pdf>

Table I:

Parameters and uncertainties for the fits on selected samples.

Note: Uncertainties were not recorded for all parameters on all fits.

Thickness was not measured by XRD on samples ThO2 050604-2 and ThO2 050818, because the samples were too thick, so XRD was used to take crystallography measurements instead.

The models used included an optically thick (1 mm) Si substrate, with a 2 nm SiO₂ oxide layer.

The constants for Si and SiO₂ were provided with the WVASE software. The ThO₂ layer was modeled with a “General Oscillator” layer originally set to the thickness estimated from XRD. A final “srough” roughness layer was added in several cases, set to the rms roughness found by AFM.

Sample ThO2 050818 was the only sample that was fit using two Tauc-Lorentz oscillators. The second oscillator was necessary to model the drop in absorption after about 6.2 eV

Sellmeier Model:

$\epsilon_{n_pole} = \frac{A_n}{E_n^2 - E^2}$, where A_n is the pole magnitude, and E_n is the pole position. The *el Offset*

term is a purely real part added to the sum of the ϵ_n terms. It effectively gives an ϵ_∞ .

Tauc-Lorentz Oscillator Model:

$\epsilon_{n_TL} = \epsilon_{n1} + i\epsilon_{n2}$, where

$$\epsilon_{n2} = \frac{A_n(E - Eg_n)^2}{(E^2 - En_n)^2 + C_n^2} \cdot \frac{\Theta(E - Eg_n)}{E}, \quad \epsilon_{n1} = \frac{2}{\pi} P \int_{R_g}^{\infty} \frac{\xi \epsilon_{n2}(\xi)}{\xi^2 - E^2} d\xi^*$$

and Θ is the Heaviside function, A represents an oscillator amplitude, Eg represents an energy cutoff for ϵ_n (the optical gap of the solid, and P is the Cauchy Principle Value.

* “In WVASE[®], this Kramers-Kronig integration is solved analytically (as in Jellison & Modine). The integral form is presented here for the sake of brevity.” [16]

Comment [MD4]: [Is this clear?](#)

	ThO2 Sample #			
	050604	050604-2	050818	
Bias Voltage (V)	64	0	65	
Other Instruments				
Crystal Monitor Thickness (nm)	50.4	808.4	N/A	
XRD Thickness (nm)	15	N/A	N/A	
AFM RMS Roughness (nm) (Two measurements per sample)	N/A	5.56 5.73	4.91 4.81	
Ellipsometer -- 2nd Fit b -- on si				
Thickness (nm)	24 ±	357 ±	578 ±	
MSE	0.0154	0.149	0.00491	
	2.47	4.702	11.22	
Sellmeier Model				
Pole 1	12.742 ± 0.000683	10.211 ± 0.0142	14.789 ± 0.0405	
Mag 1	425.7 ± 0.275	185.16 ± 1.55	259.5 ± 0.357	
Pole 2	6.426 ± 0.00197	6.5783 ± 0.0197	20.518 ± 0.373	
Mag 2	0.55999 ± 0.0432	4.1864 ± 0.855	196.19 ± 0.27	
e1 Offset	0 ± 0.0034	1.2051 ± 0.00812	1.1754 ± 0.0123	
Egap	0	0	0	
Tauc-Lorentz Oscillators				
A	4.5571 ± 117	1.7256 ± 0.343	4.328 ± 0.585	(2nd Oscillator: ThO2 050818) -14.755 ± 13.9
En	7.8795 ± 11	6.9289 ± 0.0519	6.85497	6.5032
C		0.82575 ± 16.6	0.85549 ± 0.156	0.21944 ± 0.0483
Eg	0.0001 ± 5.8	1.3554 ± 0.104	0.0001 ± 0.434	5.776 ± 0.307
n @ 2.5 eV	1.8399	1.8404	1.8867	
k @ 2.5 eV	0.0064521	0.0008329	0.0010975	

List of Figure Captions:

Figure 1: Counts per second of scattered x-rays with 2θ -angle from XRD with background noise removed. The first set of values above each peak is peak position data, with the distance between lattice planes in the middle entry. The second set of values is the standard positions and relative intensities of appropriate lattice planes for ThO_2 powder. The third set of entries shows the relative intensities of the measured peaks, normalized to the first peak.

Figure 2: Graph of composition as a function of sputtering time on sample ThO2 050604-2 as measured by XPS.

Figures 3a & 3b: Showing the surface topography for samples ThO2 050818 on the left (a), and ThO2 050604-2 on the right (b). These samples were measured to have thicknesses of 578 and 357 nm and were sputtered at 65 and 0 V, respectively.

Figure 4: Reported values of the index of refraction for seven samples. The legend shows thickness as measured by ellipsometry, and the bias voltage at which each sample was sputtered.

Figure 5: Reported values of n with photon energy over the range 3.0 to 5.0 eV. Notice that over this range, the values fall into three distinct bands. The legend labels each of the seven samples by the sample thickness as measured by ellipsometry, the bias voltage at which it was sputtered, and the band into which the sample falls. The values of n reported by Heather Liddell (1974) are also included for comparison.[10]

Figure 6: Showing average n and standard deviations at different energies. Each major division represents a different energy. The first item in the division is the average for all the samples at that energy with the standard deviation shown as error bars. The second and third items are the average values of n for the biased and unbiased samples respectively, each with their standard deviations. The fourth and fifth items show the average values of n and standard deviations for the thick samples ($d \geq 50$ nm) and the thin samples ($d < 50$ nm), respectively.

Figure 7: Plots showing n and k for two different fits on the same sample. The first fit of n was done assuming no absorption. The second fit of n was done after fitting the absorption. Note how n did not change much after adding absorption.

Figures:

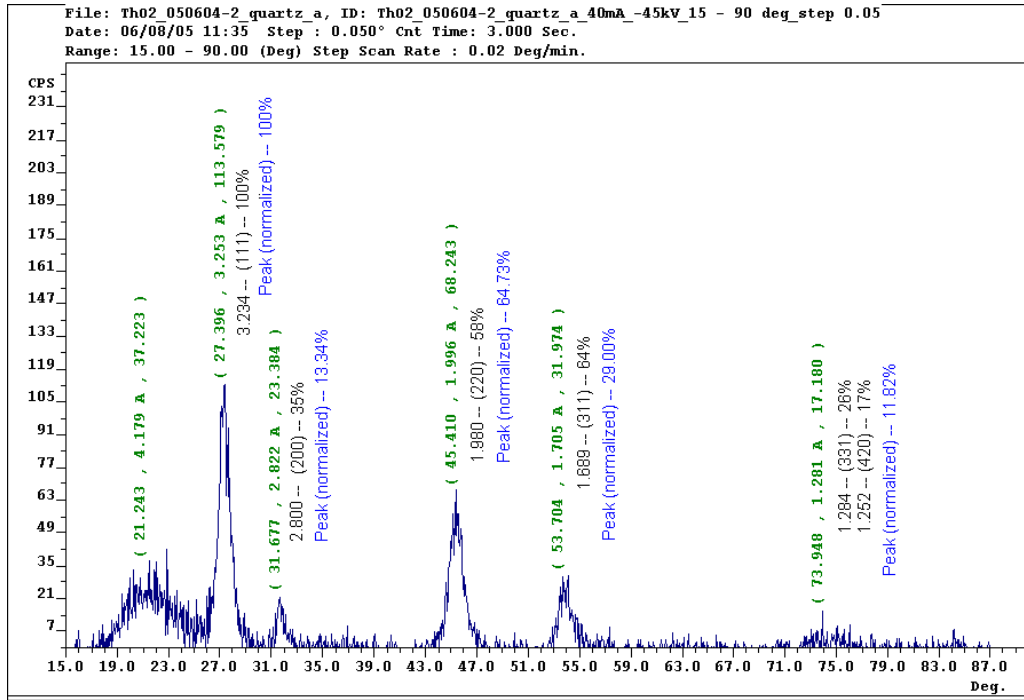


Figure 1

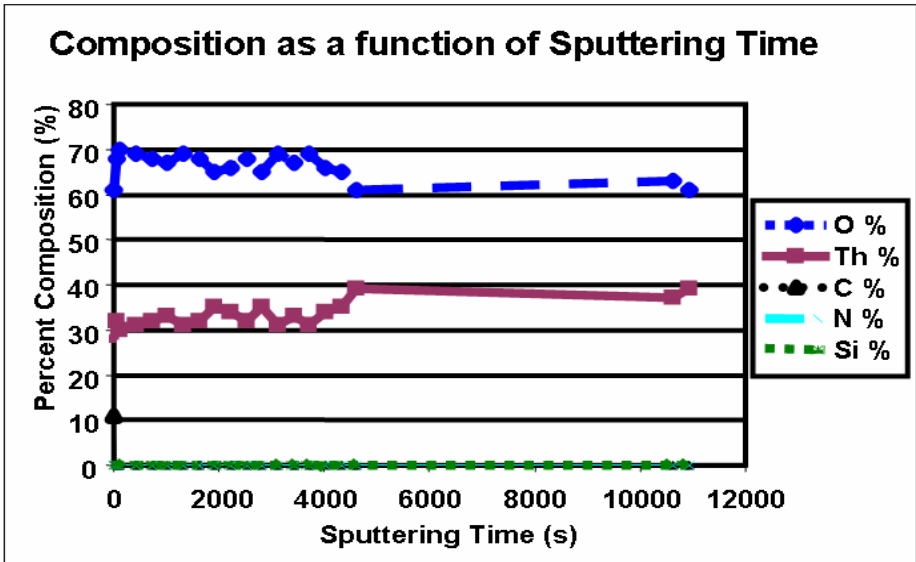


Figure 2

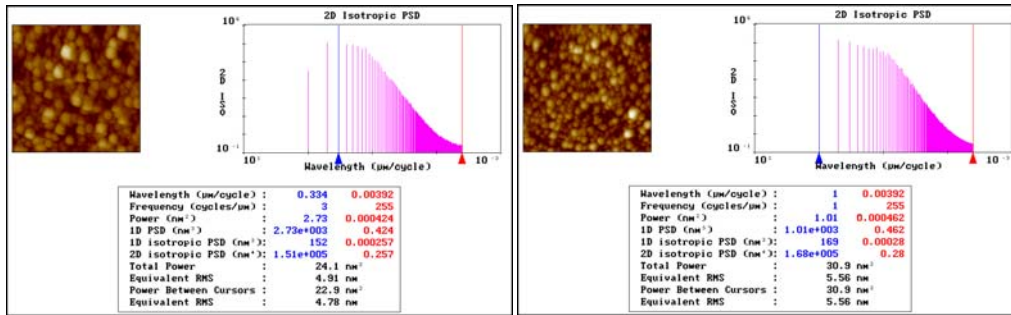


Figure 3

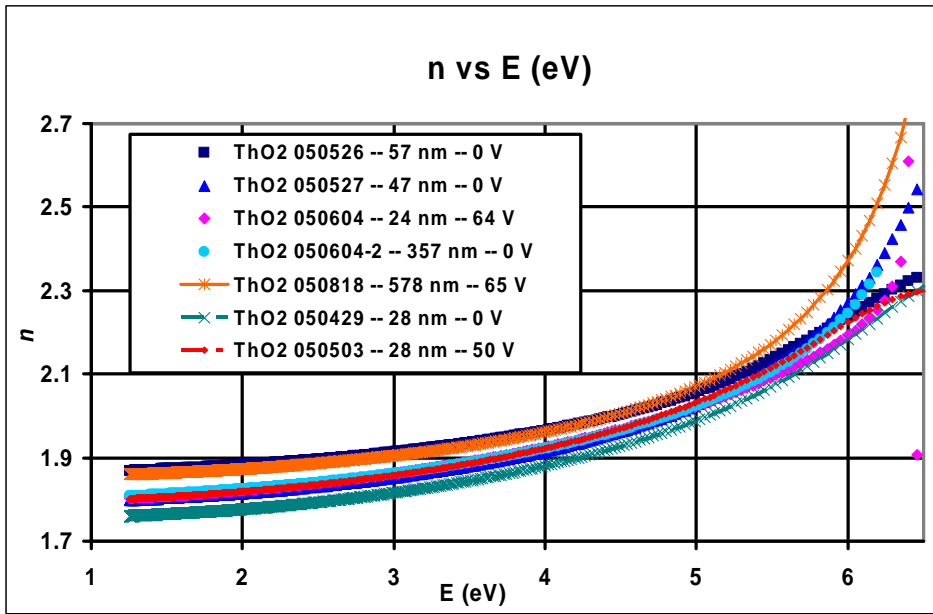


Figure 4

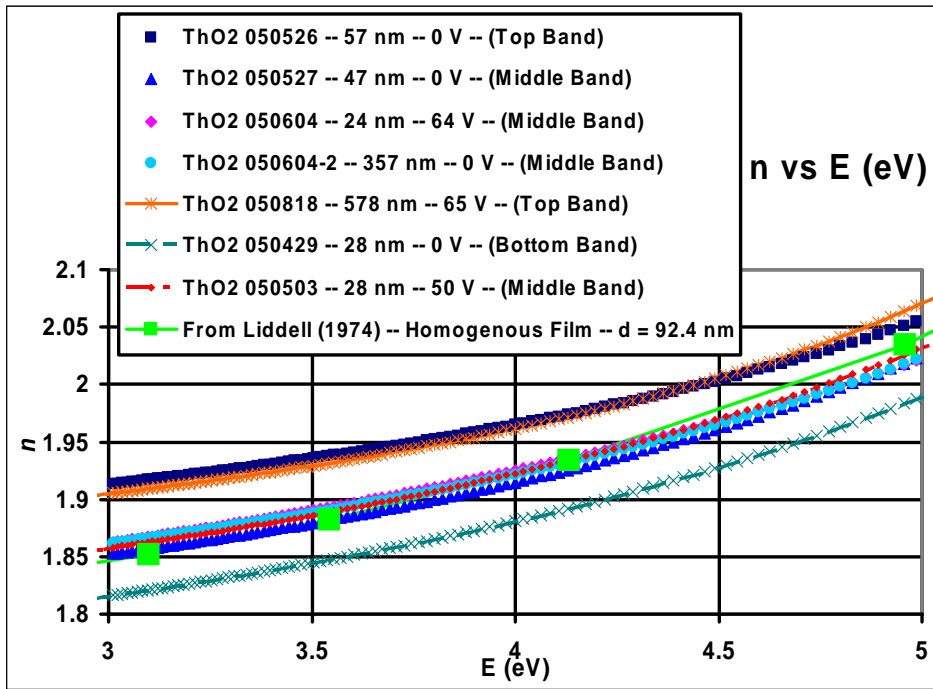


Figure 5

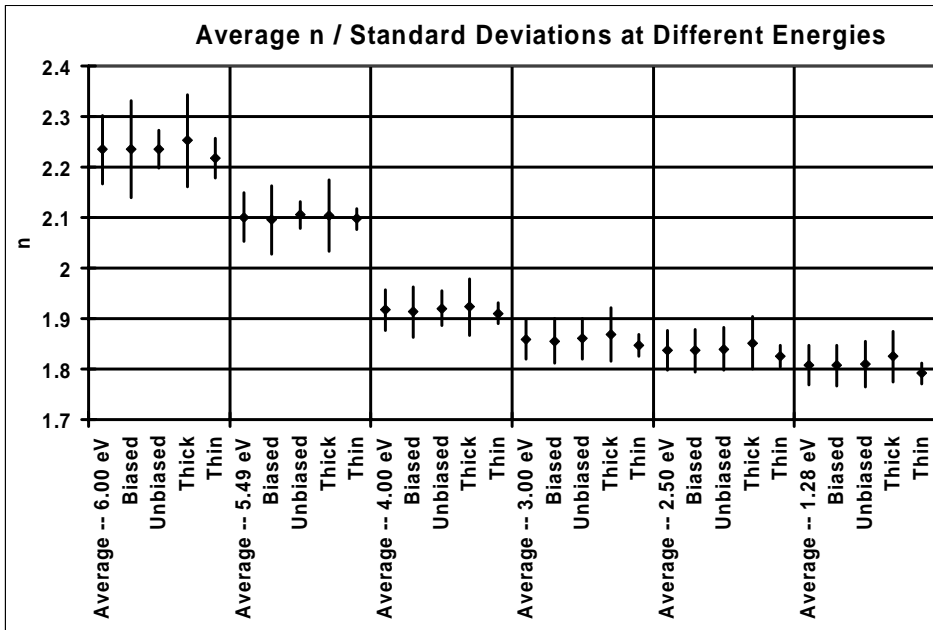


Figure 6

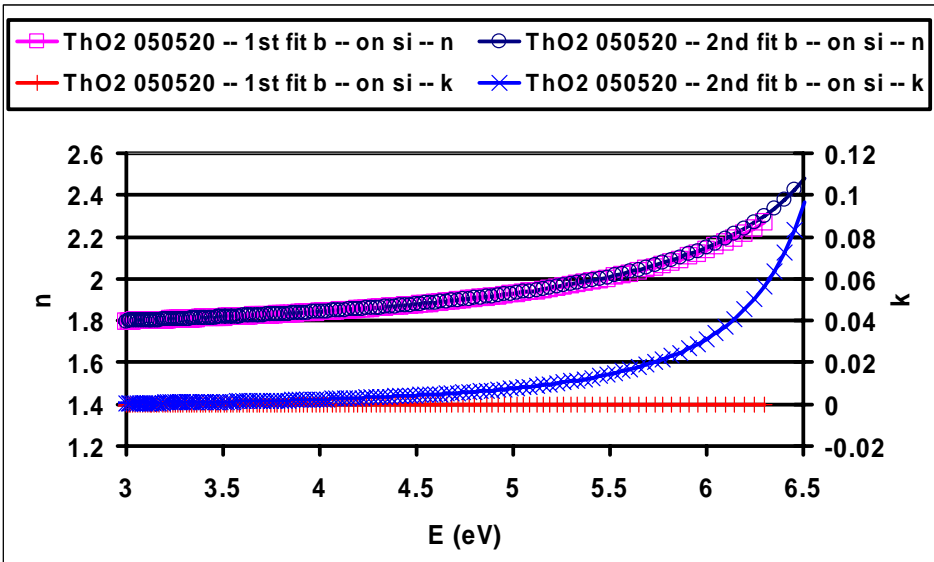


Figure 7